Inorg. Chem. **2005**, *44*, 4270–4275

Syntheses, Structures, Photoluminescence, and Theoretical Studies of a Class of Beryllium(II) Compounds of Aromatic N,O-Chelate Ligands

Yi-Ping Tong,[†,‡] Shao-Liang Zheng,*[,†] and Xiao-Ming Chen*[,†]

School of Chemistry and Chemical Engineering, Sun Yat-Sen University, Guangzhou 510275, P. R. China, and Department of Chemistry, Hanshan Normal College, Chaozhou, Guangdong 521041, P. R. China

Received January 23, 2005

Three members of a new class of luminescent, neutral, and monomeric Be(II) complexes of aromatic N,O-chelate ligands, namely $[Be(pbm)_2]$ (**1**), $[Be(pbx)_2]$ (**2**), and $[Be(pbt)_2]$ (**3**) [Hpbm = 2-(2′-hydroxylphenyl)benzimidazole, Hpbx = 2-(2′-hydroxylphenyl)benzoxazole, and Hpbt = 2-(2′-hydroxylphenyl)benzothiazole], have been prepared and characterized by X-ray crystallography and photoluminescence studies. All the complexes are neutral, mononuclear molecules and display strong photoluminescence in the blue/green region, and thus, they may serve as candidates for electroluminescence materials. The electronic transitions in the photoluminescent process have also been investigated by means of time-dependent density functional theory (TDDFT) energy level and molecular-orbital analyses, showing that their absorption and luminescent properties are ligand-based and ligand-tunable.

Introduction

The design and fabrication of efficient light-emitting devices based on organic materials have been areas of active research due to their possible applications in large area display technology.[1,2] Neutral coordination compounds are usually required since they may possess important characteristics for the performance of their electroluminescent (EL) properties, such as relatively high glass-state transition temperature and thermal stability, easy sublimation, and thin film-forming nature in a vacuum condition.[3] On the basis of the N- and/or O-donor ligands, some Al(III), B(III), and d^{10} metal complexes have shown excellent light-emitting nature and sublimation properties under vacuum condition and, therefore, can be used as EL emitters in organic diodes.[2,4−6] Similarly, Be(II) complexes, such as $[Be(bq)_2]$ (Hbq = 10-hydroxybenzo[*h*]quinoline), are considered as excellent emitting materials for organic EL devices, although such study is still sporadic.[7,8]

Due to the absence of corresponding structures and/or excited states from molecular orbital (MO) calculations, few systematic investigations on the relation between the structures and luminescent properties have been carried out;[2,4−6] therefore, the rational design and synthesis of EL emitters featuring the given emission properties are still challenging. We recently reported a class of blue/green light luminescent d^{10} metal complexes containing a new N,O-donor ligand, Hophen (Hophen = 1*H*-[1,10]phenanthrolin-2-one), and the relation between the molecular structure and the luminescence properties with the help of X-ray single-crystal structural analyses and MO calculations, showing that the photoluminescent properties can be tuned upon ligation to different metal ions.[4] On the other hand, it has been shown in the previous reports[3,5] that the benzimidazole-based derivatives are a novel class of N,O-donor ligands that could form sublimable luminescent complexes as possible EL materials. Similarly, luminescent properties of the homolo-

* Authors to whom correspondence should be addressed. E-mail: cescxm@zsu.edu.cn (X.-M.C.). Fax: int code +86 20 8411-2245 (X.-M.C.).
† Sun Yat-Sen University.
‡ Hanshan Normal College.

(1) (a) Tang, C. W.; VanSlyke, S. A. *Appl. Phys. Lett.* **1987**, *51*, 913. (b) Tang, C. W.; VanSlyke, S. A.; Chen, C. H. *J. Appl. Phys.* **1989**, *65*, 3610. (c) Wang, S.-N. *Coord. Chem. Rev.* **2001**, *215*, 79, and references cited therein.
(2) Sapochak, L. S.; Benincasa, F. E.; Schofield, R. S.; Baker, J. L.; Riccio, K. K. C.; Fogarty, D.; Kohlmann, H.; Ferris, K. F.; Burrows, P. E. *J. Am. Chem. Soc.* **2002**, *124*, 6119.
(3) Nalwa, H. S., Rohwer, L. S., Heeger, A. J., Eds. *Handbook of Luminescence, Display Materials, and Devices*; American Scientific Publishers: Stevenson Ranch, CA, 2003; and references cited therein.
(4) Zheng, S.-L.; Zhang, J.-P.; Chen, X.-M.; Huang, Z.-L.; Lin, Z.-Y.; Wong, W.-T. *Chem.—Eur. J.* **2003**, *9*, 3888.
(5) Tong, Y.-P.; Zheng, S.-L.; Chen, X.-M. Unpublished results.
(6) Yu, G.; Yin, S.; Liu, Y.; Shuai, Z.; Zhu, D. *J. Am. Chem. Soc.* **2003**, *125*, 14816.
(7) (a) Li, Y.; Liu, Y.; Bu, W.; Lu, D.; Wu Y.; Wang, Y. *Chem. Mater.* **2000**, *12*, 2672. (b) Hamada, Y.; Sano, T.; Fujita, M.; Fujii, T.; Nishio, Y.; Shibata, K. *Chem. Lett.* **1993**, 905. (c) Hamada, Y.; Sano, T.; Fujii, H.; Nishio, Y.; Takahashi, H.; Shibata, K. *Appl. Phys. Lett.* **1997**, *71*, 3338.
(8) Liu, S.-F.; Wu, Q.; Schmider, H. L.; Aziz, H.; Hu, N.-X.; Popović, Z.; Wang, S. *J. Am. Chem. Soc.* **2000**, *122*, 3671.

10.1021/ic0501059 CCC: $30.25
Published on Web 05/17/2005

Chart 1. Homologous Ligands, Where X = NH, O, and S for Hpbm, Hpbx, and Hpbt, Respectively

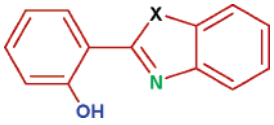

gous ligands bearing different heteroatoms (NH, O, and S) in the aromatic rings (Chart 1) can be expected. In this paper, we report the syntheses, crystal structures, and luminescent properties of three neutral, monomeric Be(II) complexes of aromatic N,O-chelate ligands, namely $[Be(pbm)_2]$ (**1**), $[Be(pbx)_2]$ (**2**), and $[Be(pbt)_2]$ (**3**) [Hpbm = 2-(2′-hydroxylphenyl)benzimidazole, Hpbx = 2-(2′-hydroxylphenyl)benzoxazole, and Hpbt = 2-(2′-hydroxylphenyl)benzothiazole]. The electronic transitions in the photoluminescent process, as well as the spectral variations along with the effect of Be(II) complexation and/or substitution effect of different heteroatoms, have been studied by means of time-dependent density functional theory (TDDFT) calculations.

Experimental Section

Materials and Physical Measurements. All reactants and solvents were purchased commercially and were used without further purification, unless otherwise stated. The organic compounds Hpbx and Hpbt were purchased from Aldrich and Acros, respectively, while Hpbm was synthesized on the basis of the literature.[9]

The C, H, and N microanalyses were carried out with an Elementar Vario E1 Elemental analyzer. ^{1}H NMR data were recorded with a Varian INOVA500NB spectrometer. The FTIR spectra were recorded using a Bruker Vector22 spectrometer in the KBr pellets in the range 4000−400 cm^{-1}. The UV−vis spectra were recorded using Varian Cary-100 spectrometer. The steady-state fluorescence and fluorescence lifetimes were determined with an Edinburgh Instrument FLS920 fluorescence spectrophotometer using a laser light resource. The FAB-MS spectrum was carried out with a high-resolution Finnigan MAT95 mass spectrometer. Thermogravimetric data (TGA) were collected on a Perkin-Elmer TGS-2 analyzer in flowing dinitrogen at a heating rate of 10 °C min^{-1} by heating microcrystals.

Synthesis and Characterization. Ligand. Hpbm was synthesized on the basis of a literature method[9] in a yield ca. 10%. Mp: 238−240 °C. FAB-MS [*m*/*z* (%)]: 211 (100.0), $[M + 1]^+$. ^{1}H NMR (DMSO-d_6; δ, ppm): 13.13 (1H, s), 13.12 (1H, s), 8.04 (1H, dd, J = 1.50, 8.00 Hz), 7.71 (1H, d, J = 8.00 Hz), 7.60 (1H, d, J = 7.50 Hz), 7.38 (1H, m), 7.28 (2H, m), 7.03 (2H, m). Anal. Calcd for $C_{13}H_{10}N_2O$: C, 74.27; H, 4.79; N, 13.33. Found: C, 74.02; H, 4.81; N, 13.49. FTIR (KBr): 3326 vs, 1585 s, 1492 s, 1417 s, 1320 m, 1282 m, 1262 s, 1133 m, 1037 w, 911 w, 840 w, 798 w, 727 m, 591 w, 522 w, 464 w cm^{-1}.

$[Be(pbm)_2]$ (1). To a filtered solution of Hpbm (0.42 g, 2 mmol) in ethanol (40 mL) at a temperature of 60 °C was added a filtered solution of $BeSO_4{\cdot}4H_2O$ (0.18 g, 1 mmol) in ethanol (80 mL). The mixture was kept for 6 h at this temperature and allowed to stand overnight at room temperature. The white precipitate was filtered off, washed with ethanol, and dried under reduced atmosphere over silica gel at 50 °C for 3 h. The product was obtained in 75% yield. The colorless crystals for X-ray work were grown by very slow evaporation of a DMF solution of **1** for ca. 3 months. Anal. Calcd for $C_{26}H_{18}BeN_4O_2$: C, 73.05; H, 4.24; N 13.11. Found: C, 72.95; H, 4.18; N, 13.08. ^{1}H NMR (DMSO-d_6; δ, ppm): 13.45 (2H, s), 8.08 (2H, dd, J = 2.00, 8.50 Hz), 7.54 (2H, d, J = 8.00 Hz), 7.35 (2H, m), 7.17 (2H, m), 6.95 (2H, m), 6.79 (4H, t, J = 6.79, 7.50 Hz), 6.72 (2H, d, J = 7.72 Hz). FTIR (KBr): 3058 m, 1625 w, 1605 m, 1561 m, 1540 m, 1486 s, 1450 m, 1310 m, 1263 s, 1164 w, 1146 s, 1098 w, 1042 m, 1016 w, 894 s, 831 w, 773 m, 745 s, 619 m, 567 m, 481 m cm^{-1}.

$[Be(pbx)_2]$ (2). To a filtered solution of Hpbx (0.42 g, 2 mmol) in ethanol (50 mL) was added a filtered solution of $BeSO_4{\cdot}4H_2O$ (0.18 g, 1 mmol) and triethylamine (0.88 g, 8.7 mmol); the mixture was stirred at 60 °C for 3 h and then was allowed to stand at room temperature for 3 days, yielding white crystals. The yield was 0.35 g (81.5%). X-ray-quality crystals were obtained by very slow evaporation of an acetone solution of **2** for ca. 70 days. Anal. Calcd for $C_{26}H_{16}BeN_2O_4$: C, 72.72; H, 3.76; N, 6.52. Found: C, 72.58; H, 3.85; N, 6.53. ^{1}H NMR (DMSO-d_6; δ, ppm): 8.06 (2H, dd, J = 1.50, 8.00 Hz), 7.86 (2H, d, J = 8.50 Hz), 7.54 (2H, m), 7.39 (2H, m), 7.23 (2H, ddd, J = 1.00, 7.50, 8.00 Hz), 6.91 (6H, m). FTIR (KBr): 1621 s, 1538 s, 1476 s, 1440 m, 1373 w, 1340 m, 1275 s, 1187 w, 1157 w, 1135 w, 1069 w, 1030 w, 999 w, 913 s, 774 m, 747 s, 705 m, 664 w, 617 w, 561 w, 466 w cm^{-1}.

$[Be(pbt)_2]$ (3). To a filtered solution of Hpbt (0.45 g, 2 mmol) was added a filtered solution of $BeSO_4{\cdot}4H_2O$ (0.18 g, 1 mmol) and triethylamine (0.53 g, 5.23 mmol) in ethanol (50 mL). The mixture was stirred at 60 °C for 2 h and allowed to stand at room temperature overnight, yielding **3** as yellowish microcrystals. The yield was 0.32 g (70%). Anal. Calcd for $C_{26}H_{16}BeN_2O_2S_2$: C, 67.66; H, 3.49; N, 6.07. Found: C, 67.64; H, 3.40; N, 6.13. ^{1}H NMR (DMSO-d_6; δ, ppm): 8.15 (2H, d, J = 8.00 Hz), 7.91 (2H, d, J = 8.00 Hz), 7.47 (2H, t, J = 7.50 Hz), 7.35 (2H, m), 7.26 (2H, t, J = 8.00 Hz), 7.04 (2H, d, J = 4.00 Hz), 6.86 (4H, t, J = 8.50 Hz). FTIR (KBr): 1609 m, 1548 m, 1493 s, 1472 s, 1426 m, 1341 m, 1252 m, 1232 m, 1156 w, 932 m, 751 m, 602 m cm^{-1}. X-ray-quality crystals were grown by heating a mixture of $BeSO_4{\cdot}4H_2O$ (0.142 g, 0.1 mmol) and Hpbt (0.045 g, 0.2 mmol) in ethanol (13 mL), which was sealed in a 23-mL Teflon-lined stainless steel container at 110 °C for 7 days; after the sample was cooled to room temperature at a rate of 5 K/h, yellowish block crystals of **3** were isolated.

Calculation Details. All the calculations were performed with Gaussian03 suite of programs.[10] The geometric optimizations were carried out on the 6-31G** basis sets for all atoms and B3LYP level (for selected optimized geometric parameters, see Table S1). The TDDFT calculations were employed to calculate the excited states and electronic spectra at the B3LYP level with 6-31G** basis sets for all atoms. The electron density diagrams of molecular orbitals were obtained with the Molden 3.5 graphics program.

X-ray Crystallography. Diffraction intensities for **1**−**3** were collected at 293 K on a Bruker Smart Apex CCD diffractometer (Mo Kα, λ = 0.710 73 Å). The structure was solved by direct methods and refined with a full-matrix least-squares technique using

(9) Addison, A. W.; Burke, P. J. *J. Heterocycl. Chem.* **1981**, *18*, 803.

(10) Frisch, M. J.; Trucks, G. W.; Schlegel, H. B.; Scuseria, G. E.; Robb, M. A.; Cheeseman, J. R.; Zakrzewski, V. G.; Montgomery, J. A.; Stratmann, R. E.; Burant, J. C.; Dapprich, S.; Millam, J. M.; Daniels, A. D.; Kudin, K. N.; Strain, M. C.; Farkas, O.; Tomasi, J.; Barone, V.; Cossi, M.; Cammi, R.; Mennuci, B.; Pomelli, C.; Adamo, C.; Clifford, S.; Ochterski, J.; Petersson, G. A.; Ayala, P. Y.; Cui, Q.; Morokuma, K.; Malick, D. K.; Rabuck, A. D.; Raghavachari, K.; Foresman, J. B.; Cioslowski, J.; Oritz, J. V.; Stefanov, B. B.; Liu, G.; Liashenko, A.; Piskorz, P.; Komaromi, I.; Gomperts, R.; Martin, R. L.; Fox, D. J.; Keith, T.; Al-Laham, M. A.; Peng, C. Y.; Nanayakkara, A.; Gonzalez, C.; Challacombe, M.; Gill, P. M. W.; Johnson, B. G.; Chen, W.; Wong, M. W.; Andres, J. L.; Head-Gordon, M.; Replogle, E. S.; Pople, J. A. *GAUSSIAN03*, revision C.02; Gaussian, Inc.: Pittsburgh, PA, 2003.

Table 1. Crystal and Structure Refinement Data for **1**−**3**

param	**1**	**2**	**3**
chem formula	$C_{26}H_{18}BeN_4O_2$	$C_{26}H_{16}BeN_2O_4$	$C_{26}H_{16}BeN_2O_2S_2$
fw	427.45	429.42	461.54
temp, K	293(2)	293(2)	293(2)
cryst system	tetragonal	orthorhombic	monoclinic
space group	$P4_32_12$	*Pbca*	*C*2/*c*
a, Å	9.6525(3)	10.283(1)	24.525(2)
b, Å	9.6525(3)	16.755(1)	12.058(1)
c, Å	22.477(2)	24.935(2)	14.796(1)
β, deg	90	90	93.414(1)
V, Å^3	2094.2(2)	4295.8(6)	4367.9(5)
Z	4	8	8
μ(Mo Kα), mm^{-1}	0.087	0.090	0.271
ρ_{calcd}, g cm^{-3}	1.356	1.328	1.404
R1 [$I > 2\sigma(I)$][a]	0.0425	0.0641	0.0445
wR2 [$I > 2\sigma(I)$][a]	0.1072	0.1098	0.1182
R1 (all data)[a]	0.0524	0.1290	0.0578
wR2 (all data)[a]	0.1134	0.1312	0.1285

[a] $R1 = \sum||F_o| - |F_c||/\sum|F_o|$, $wR2 = [\sum w(F_o^2 - F_c)^2/\sum w(F_o^2)^2]^{1/2}$.

Table 2. Selected Bond Lengths (Å) and Bond Angles (deg) for **1**−**3**[a]

	Compound **1**		
Be(1)−O(1)	1.598(3)	Be(1)−N(1)	1.698(3)
O(1)−Be(1)−O(1A)	115.3(3)	O(1)−Be(1)−N(1A)	110.6(1)
O(1)−Be(1)−N(1)	103.9(1)	N(1)−Be(1)−N(1A)	113.0(2)
	Compound **2**		
Be(1)−O(1)	1.574(3)	Be(1)−N(1)	1.730(3)
Be(1)−O(2)	1.572(3)	Be(1)−N(2)	1.727(3)
O(2)−Be(1)−O(1)	117.9(2)	O(2)−Be(1)−N(1)	110.7(2)
O(2)−Be(1)−N(2)	104.0(2)	O(1)−Be(1)−N(1)	103.6(2)
O(1)−Be(1)−N(2)	109.1(2)	N(2)−Be(1)−N(1)	111.8(2)
	Compound **3**		
Be(1)−O(1)	1.560(3)	Be(1)−N(1)	1.754(3)
Be(1)−O(2)	1.578(3)	Be(1)−N(2)	1.750(3)
O(2)−Be(1)−O(1)	116.1(2)	O(2)−Be(1)−N(1)	111.2(2)
O(2)−Be(1)−N(2)	103.9(1)	O(1)−Be(1)−N(1)	105.6(1)
O(1)−Be(1)−N(2)	112.0(2)	N(2)−Be(1)−N(1)	107.8(1)

[a] Symmetry codes for **1**: (A) $y + 1$, $x - 1$, $-z$.

the SHELXTL program package.[11] Anisotropic thermal parameters were applied to all non-hydrogen atoms. The organic hydrogen atoms were generated in the calculated positions. Crystal data and details of data collection and refinements are summarized in Table 1. Selected bond lengths and bond angles are listed in Table 2. CCDC reference numbers 240085−240087 are for **1**−**3**, respectively. These data can be obtained free of charge via www.ccdc.cam.ac.uk/conts/retrieving.html (or from the Cambridge Crystallographic Data Center, 12 Union Road, Cambridge CB2 1EZ, U.K.; fax (+44) 1223-336-033; deposit@ccdc.cam.uk).

Results and Discussion

Synthesis. Similar to the neutral coordination compounds for EL materials,[2] the single crystals of **1**−**3** for X-ray diffraction were hard to grow, although their solids can be prepared by mixing the solutions of beryllium sulfate and corresponding ligands at 1:2 ratio in ethanol. Fortunately, X-ray-quality crystals of the neutral, mononuclear molecules were obtained after many trials using different ways including conventional, diffusion, and hydrothermal methods; thus, the systematic investigations of their luminescence properties could be carried out. This work implies that the crystallization condition is important.

For comparison of the spectroscopic properties, the crystals of Hpbm,[12] Hpbx,[13] and Hpbt[14] were also grown from open solutions, characterized by X-ray crystallography, and examined spectroscopically.

Thermal stabilities of the powders of **1**−**3** were characterized by thermogravimetric measurements (Figure S1). As expected, they exhibit high thermal stability with decomposition temperatures of 514, 392, and 406 °C for **1**−**3**, respectively, which are comparable to those of EL materials of $[Zn(BTZ)_2]_2$[6] (HBTZ = 2-(2′-hydroxylphenyl)benzothiazole) and $[Znq_2]_4$[2] and imply the solid samples should be sublimable under vacuum.

Descriptions of Crystal Structures. Although **1**−**3** crystallize in different space groups (Table 1), the Be(II) ion in each compounds is coordinated by two deprotonated ligands and located in a slightly distorted tetrahedral geometry (Figure 1). The Be−O distances are 1.598(3), 1.574(3)/1.572(3), and 1.560(3)/1.578(3) Å, while Be−N distances are 1.698(3), 1.730(3)/1.727(3), and 1.754(3)/1.750(3) Å for **1**−**3**, respectively (see Table 2), which fall in the typical Be−O lengths (1.56−1.63 Å) or Be−N lengths (1.65−1.80 Å).[7,8] The fact is that the Be−N length variation along with the different substitution effects of heteroatoms (NH, O, and S) favors the increasing orderly trend of the negative charge density for the deprotonated ligand in the complexes. The N−Be−N and O−Be−O bond angles of 107.8(1)−113.0(2) and 115.3(3)−117.9(2)° are all typical values for tetrahedral geometry. The dihedral angles between two chelated ligand planes of ca. 87−90° indicate that they are slightly distorted from an ideal tetrahedral geometry.

We noted that intramolecular hydrogen bonds in the neutral ligands Hpbm, Hpbx, and Hpbt are all observed between the phenolic OH group and the N atom of heterocyclic ring with corresponding O···N distances of 2.554(2), 2.705(7), and 2.610(3) Å,[15] respectively, resulting in the planar structures (Figure S2). Similar to the corresponding ligands, the dihedral angles between the phenolate and heterocycle moieties of **1**−**3** are less than 10°, featuring a basically planar fashion.

Different supramolecular interactions, such as hydrogen bonding and/or $\pi-\pi$ stacking interactions, play a very important role in construction of the three-dimensional architectures. In **1**, the imidazole group donates a hydrogen

(11) Sheldrick, G. M. *SHELXTL 6.10*; Bruker Analytical Instrumentation: Madison, WI, 2001.

(12) Crystal data for Hpbm: orthorhombic, space group *Pnma*; M_r = 210.23; a = 18.236(16), b = 4.8061(17), c = 11.990(11) Å; V = 1050.8(14) Å^3; Z = 4; R_1 [$I \geq 2\sigma(I)$] = 0.0425, wR_2 (all data) = 0.1057, Goof = 1.041, in ref 5.

(13) Crystal data for Hpbx: orthorhombic, space group *Pnma*; M_r = 211.21; a = 22.446(3), b = 11.5504(15), c = 3.8547(5) Å; V = 999.4(2) Å^3; Z = 4; R_1 [$I \geq 2\sigma(I)$] = 0.0558, wR_2 (all data) = 0.1403, Goof = 1.108.

(14) Crystal data for Hpbt: monoclinic, space group $P2_1/c$; M_r = 227.27; a = 12.4088(16), b = 5.8502(8), c = 15.639(2) Å; β = 111.663(2)°; V = 1055.1(2) Å^3; Z = 4; R_1 [$I \geq 2\sigma(I)$] = 0.0688, wR_2 (all data) = 0.1962, Goof = 1.051. These data are similar to that in the following: Aydin, A.; Soylu, H.; Akkurt, M.; Arici, C.; Erdemir, M. *Z. Kristallogr.—New Cryst. Struct.* **1999**, *214*, 529.

(15) Note that, in the structure of Hpbt reported in ref 14, the location of hydrogen atom in OH group may be controversial, as the intramolecular hydrogen bond is more reasonable based on the difference Fourier map and in agreement with the presence of excited-state intramolecular proton transfer (ESIPT, mentioned below).

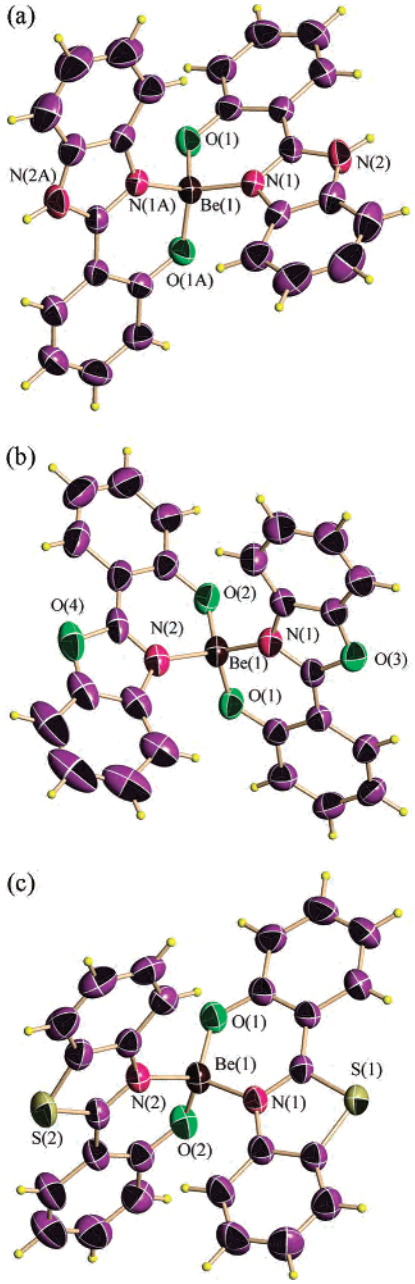

Figure 1. Perspective views of coordination structures in **1** (a), **2** (b), and **3** (c). Thermal ellipsoids are plotted at the 50% probability level. Symmetry code for **1**: (A) $y + 1, x - 1, -z$.

bond to the phenolate O atom of an adjacent molecule [N(2A)···O(1) 2.849(2) Å], resulting in a three-dimensional supramolecular array. There are weak intermolecular C−H···O hydrogen bonds [C···O 3.386(3) Å] in **2**. However, no intermolecular hydrogen-bonding interaction exists in the structure of **3** (Figure 2). On the other hand, although $\pi-\pi$ interaction is absent in the structure of **1**, offset $\pi-\pi$ stacking interactions (ca. 3.38 Å) involving the phenolate ring atoms and the benzoxazole moieties of adjacent molecules exist in **2**, while offset $\pi-\pi$ stacking interactions (ca. 3.38 and 3.54 Å) between the aromatic ligands are found in **3** (Figures 3 and S3). There are also weak S···S interactions (3.62 Å, slightly shorter than twice of the van der Waals radius of sulfur atom[16]) in the supramolecular array of **3**.

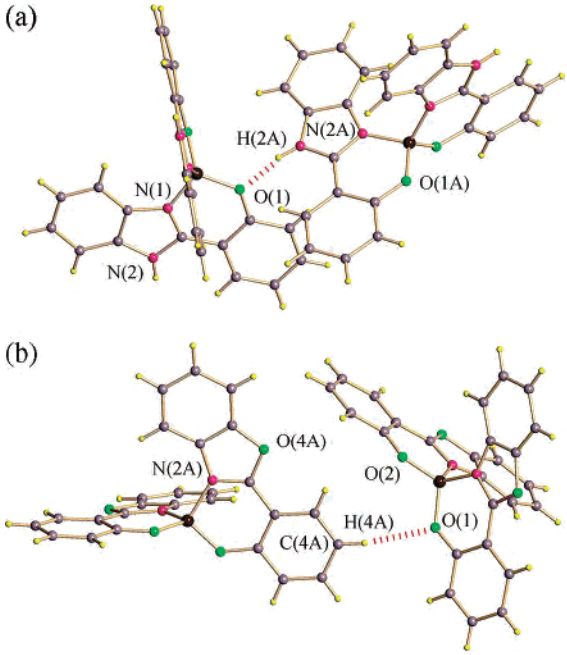

Figure 2. Perspective views of intermolecular hydrogen bonds in **1** (a) and **2** (b). Symmetry code for **1**: (A) $-y + 1/2, x + 1/2, z - 1/4$. Symmetry code for **2**: (A) $x + 1/2, -y + 1/2, -z + 1$.

Spectroscopic Properties. As shown in Table 3, the lowest energy absorption bands of powdered crystals of **1**−**3** occur at 352, 385, and 395 nm, respectively, while their corresponding ligands, Hpbm, Hpbx, and Hpbt, occur at 342, 356, and 364 nm, respectively (Figure S4).

We noted that the lowest energy absorption maximum of Hpbm is the S_0-S_1 transition, assignable to be $\pi \rightarrow \pi^*$ in nature.[5] According to our TDDFT calculations, the same process is found in those of Hpbx and Hpbt (Table 3 and Figure S5). However, the lowest energy absorption maxima in the UV spectra, in fact, may correspond to S_0-S_n transitions with $n \geq 1$, as the S_0-S_1 transition may have lower oscillator strength.[17,18] In current cases, the lowest energy absorption maxima for **1** and **2** are attributed to the S_0-S_4 transitions (calcd wavelength 338 and 343 nm, oscillator strength 0.22 and 0.18, respectively), while the lowest energy absorption maximum for **3** can be attributed to the S_0-S_3 transition (calcd wavelength 370 nm, oscillator strength 0.18), as the transitions in lower excited state−ground state (ES−GS) separations are almost forbidden. The ES−GS separations that are derived from TDDFT calculations are in agreement with those observed experimentally.

On the other hand, the S_0-S_4 transitions (lowest energy absorption maxima) for **1** and **2** are mainly associated with the transitions from the corresponding HOMO-1 to LUMO+1 (coefficients up to 0.66),[19] while for **3** the S_0-S_3 transition is mainly associated with the transition from the corresponding HOMO to LUMO+1 (coefficients up to 0.64). As shown in Figure 4, the corresponding molecular orbitals

(16) Dean, J. A. D. *Lange's Handbook of Chemistry*, 15th ed.; McGraw-Hill Book Co.: Beijing, 1999.
(17) Turro, N. J.; Liu, K.-C.; Show, M.-F.; Lee, P. *Photochem. Photobiol.* **1978**, *27*, 523.
(18) Klessinger, J. M.; Michl, J. *Excited states and photochemistry of organic molecules*; VCH: New York, 1995.

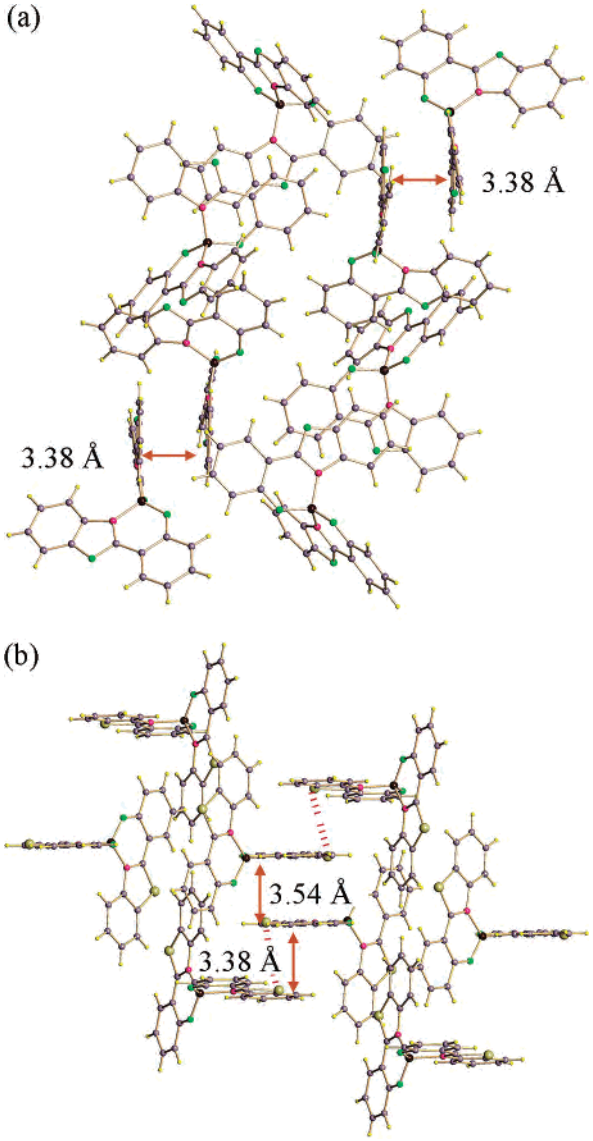

Figure 3. Perspective views of $\pi-\pi$ stacking interactions and S···S interactions (dash line) in **2** (a) and **3** (b).

Table 3. Calculated and Experimental Absorption Wavelengths (nm) and Transition Nature for **1**−**3**, Hpbm, Hpbx, and Hpbt Together with Oscillator Strengths

		wavelength		
compd	transition nature	calcd	exptl	oscillator strength
Hpbm	$\pi \rightarrow \pi^*$	313	342	0.44
Hpbx	$\pi \rightarrow \pi^*$	316	356	0.37
Hpbt	$\pi \rightarrow \pi^*$	335	364	0.34
1	$\pi \rightarrow \pi^*$	338	352	0.22
2	$\pi \rightarrow \pi^*$	343	385	0.18
3	$\pi \rightarrow \pi^*$	370	395	0.18

are mainly the π-bonding and π^*-antibonding orbitals of corresponding deprotonated ligands; therefore, such transitions can be assigned as $\pi \rightarrow \pi^*$ in nature.

As mentioned above, the Be−N bond length variation along with the different substitution effects of heteroatoms (NH, O, and S) favors the increasing trend of the negative charge density for the deprotonated ligand in **1**−**3** in order,

(19) HOMO, highest occupied molecular orbital; LUMO, lowest unoccupied molecular orbital.

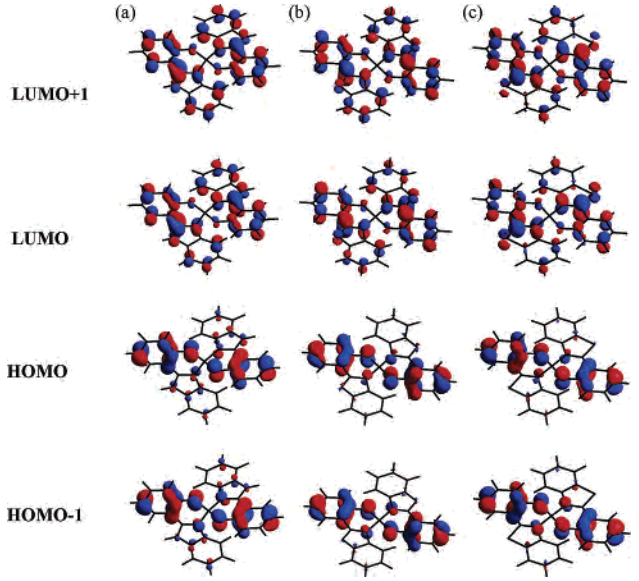

Figure 4. Contour plots of the relevant molecular orbitals (from HOMO-1 to LUMO+1) of **1** (a), **2** (b), and **3** (c).

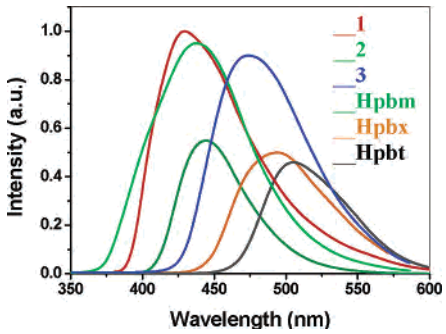

Figure 5. Emission spectra of **1**−**3**, Hpbm, Hpbx, and Hpbt in the solid state.

which results in the decreasing ES−GS separation of the relevant compound, in accordance with the results of TDDFT energy level.

It has been found that the deprotonation and coordination of organic ligands to d^{10} metal ions can significantly reduce the energy gaps between the HOMOs and LUMOs.[4,20] Such trend is also found in **1**−**3**, as the TDDFT energy levels show that the S_0-S_1 energy separations of **1**−**3** become smaller. According to the energy-gap law for radiationless deactivation,[21] the luminescence of **1**−**3** should be red-shifted compared with their corresponding ligands. However, Hpbm, Hpbx, and Hpbt emit at 444, 494, and 505 nm, respectively, while **1**−**3** emit at 428, 440, and 474 nm, respectively (Figure 5). Noted that, for Hpbm, Hpbx, and Hpbt, an extremely rapid excited-state intramolecular proton transfer (ESIPT) via a cis enol structure with intramolecular hydrogen bonding between the phenolic group and imidazole nitrogen atom is observed (Scheme 1), being manifested by the lack of the primary emission and the appearance of a strongly Stokes-

(20) (a) Zheng, S.-L.; Yang, J.-H.; Yu, X.-L.; Chen, X.-M.; Wong, W.-T. *Inorg. Chem.* **2004**, *43*, 830. (b) Zheng, S.-L.; Chen, X.-M. *Aust. J. Chem.* **2004**, *57*, 703.

(21) Turro, N. J. *Modern Molecular Photochemistry*; University Science Books: Sausalito, CA, 1991.

Scheme 1. Electronic Transitions in the Photoluminescent Process of **1**−**3** (a) and Hpbm, Hpbx, and Hpbt (b)

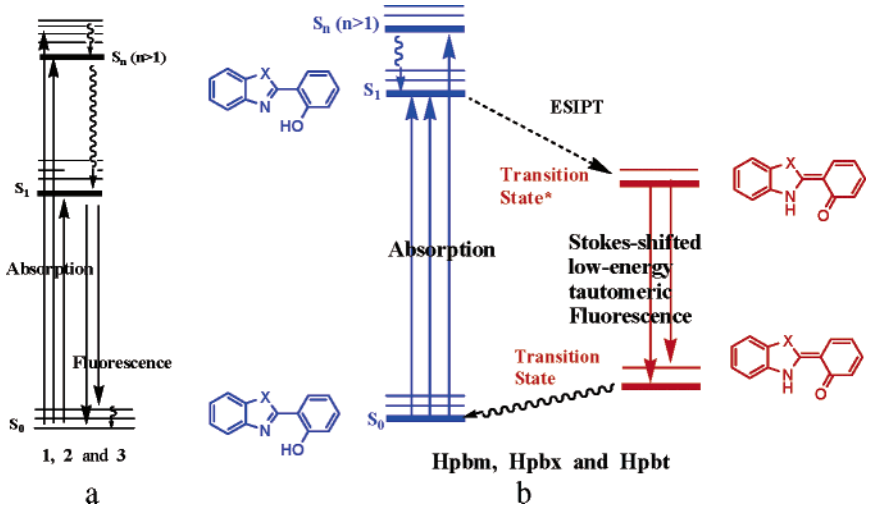

shifted low-energy tautomeric fluorescence.[22] Thus, compared with the neutral ligands, the "violation" of blue-shifts is found in the spectroscopic observations of **1**−**3**.

According to the TDDFT energy level and MO analyses, S_0-S_1 transitions of **1**−**3** are mainly associated with the transitions from the corresponding HOMOs to LUMOs (coefficients up to 0.67), in which the HOMOs are mainly the π-bonding orbitals of deprotonated ligands, while the LUMOs are the π^*-antibonding orbitals of the deprotonated ligands; thus, the luminescence originates from the $\pi \rightarrow \pi^*$ transition (LLCT). Similar to those of common d^{10} metal complexes without metal−hydroxy (or oxy) clusters,[4,5,20] the lifetimes of solids **1**−**3** are only ca. 1.38, 3.64, and 1.18 ns at room temperature, respectively (Figure S6).

The photoluminescent properties of d^{10} metal complexes can be tuned upon ligation to the metal ions with different electronegativity values.[4,20] It seem much more complex for the homologous compounds featuring different heteroatoms in the aromatic rings, as the different heteroatoms (NH, O, and S) substitution has an impact on both ΔHOMO and ΔLUMO, resulting in the complicated effect on the energy gaps between the HOMOs and LUMOs (Table S2). On the other hand, in the series of homologous compounds with only different heteroatom substitution in the same site of the aromatic ring, the magnitude of the dipole moments is variable but the orientation of the dipole moments should be conformable, which can also be verified theoretically in the current case. It is notable that the energy gaps between the HOMOs and LUMOs increase along with the enhancement of their dipole moments in the homologous compounds,[15,23] such as those with a different heteroatom (CH and N) substitution in the aromatic ring.[24] In our case, with different heteroatoms (NH, O, and S) merely substituted in the aromatic ring, the reducing dipole moments (3.75, 2.10, and 2.00 D for Hpbm, Hpbx, and Hpbt, respectively, and 4.84, 4.20, and 3.90 D for **1**−**3**, respectively) result in the decreasing ES−GS separations of relevant compounds in order, in consonance with the results of the experimental spectra and TDDFT energy levels.

Conclusions

As candidates for blue EL materials, a new class of stable, neutral, and mononuclear Be(II) complexes have been prepared. On the basis of the X-ray structures and TDDFT energy level and molecular-orbital analyses, the systematic investigation of the electronic transitions in the photoluminescent processes of all compounds have shown that their absorption and luminescent properties are ligand-based. The investigations on the relation between structures and luminescent properties further explicate the spectral variation of the effect of complexation with Be(II) cations and/or substitution of different heteroatoms (NH, O, and S) in the ligand rings. This work demonstrates that the ligand-tuning approach may be useful for the preparation of potential luminescent metal−organic materials with different emitting colors.

Acknowledgment. This work was supported by the National Natural Science Foundation of China (Grant No. 20131020), the Ministry of Education of China (Grant No. 01134), and the Scientific and Technological Project of Guangdong Province.

Supporting Information Available: Calculated molecular geometric parameters and UV−vis spectra for **1**−**3**, Hpbm, Hpbx, and Hpbt, additional plots (PDF), and X-ray data files (CIF). This material is available free of charge via the Internet at http://pubs.acs.org.

IC0501059

(22) Waluk, J. *Conformational Analysis of Molecules in Excited States*; Wiley-VCH: New York, 2000; pp 83−85 and references cited therein.

(23) For example, see the following series of papers: Michl, J. Magnetic Circular Dichroism of Cyclic π-Electron Systems (1−18). *J. Am. Chem. Soc.* **1978**, *100*, 6801−6898.

(24) The calculated dipole moments of BPh_2(2-py-in) and BPh_2(2-py-aza) in ref 8 [2-py-in = 2-(2-pyridyl)indole, 2-py-aza = 2-(2-pyridyl)-7-azaindole], in which they are different heteroatom (CH for the former and N for the latter) substitutions in the aromatic ring, are 5.29 and 6.24 D, in consonance with the results of the spectra and molecular orbital energy levels (Table S2).